ARCHIVES OF ACOUSTICS
15, 3-4 417-435 (1990)

APPLICATION OF THE ACOUSTIC EMISSION METHOD IN FATIGUE CRACKING AND FRACTURE TOUGHNESS ESTIMATION FOR STEEL

S. PILECKI*, J. SIEDLACZEK**

* Institute of Fundamental Technological Research, Polish Academy of Sciences
(00-049 Warszawa, ul. Świętokrzyska 21)
** High Pressure Research Center, Polish Academy of Sciences
(01-142 Warszawa, ul. Sokołowska 29)

The present paper consists of the confirmation of previous works where the great variety of the acoustic emission (AE) characteristics of different metals have been found. Based on the experiments conducted for the St90PA steel, possibilities of the fatigue cracks initiation detection by use of the AE method are discussed herein.. Relations between the fatigue crack length and AE count rate or count sum have been determined and the possibilities of the application of AE in fracture toughness estimation as well as in critical stress intensity factor K_{Ic} calculations have been presented. It has been stated that creation of the fatigue cracks in steel can be detected much earlier by use of the AE method than it was possible by use of the classical optical method. AE method also makes the estimation of the propagating crack length easier as well as it can make the estimation of the fracture toughness more accurate.

Kontynuując wcześniejsze prace, w których stwierdzono dużą różnorodność charakterystyk akustycznych różnych metali, w niniejszej pracy na przykładzie stali St90PA zbadano możliwości wykrywania inicjacji pęknięć zmęczeniowych metodą EA, wyznaczono zależność między długością pęknięcia zmęczeniowego a gęstością i sumą zliczeń EA oraz naświetlono możliwości wykorzystania EA w wyznaczaniu odporności na pękanie i obliczaniu wartości krytycznego współczynnika intensywności naprężeń K_{Ic}. Zostało wykazane, że powstawanie pęknięć zmęczeniowych w stali może być metodą EA wykryte znacznie wcześniej niż metodą optyczną. Metoda EA ułatwia też ocenę długości propagującego się pęknięcia, jak również może uściślić ocenę odporności na pękanie.

1. Introduction

In the case of cyclic as well as static loading the quantitative significance of results obtained in the experimental measurements carried out for given conditions can only be estimated with their reference to the acoustic characteristic of tested

material. It is well known [1] that significant differences can be observed in the case of acoustic emission (AE) of different materials and the AE measurements usually allow rather for the comparison.

2. Acoustic emission phenomenon in fatigue cracking process

The simplest relations between AE and rate of cracking were first detected in 1964 [4]. In 1967 relations between the AE count sum and load were given for aluminum alloys and steel [5]. In 1976 BAILEY et al. [8] stated that there exists a very good correlation of the AE count sum with the fatigue crack length. Relation between the strees intensity factor K and AE per unit crack length was also shown in [6, 7].

The main reference for the acoustic investigations of a given material tested for cyclic loading is its dynamic acoustic emission characteristic. Determination of the complete characteristic is a time-consuming process. It happens because this characteristic depends on many parameters, such as range and history of loading, geometry of specimen, its material proporties, kind of specimen's mechanical and heat treatment and, eventually, existence of notch. With regard to the qualitative correlation of the AE phenomenon and the cracking process of dynamically loaded material, the AE measurement allows for a more precise estimation of crack initiation and crack growth than the commonly used optical method.

Establishment of the moment of fatigue crack initiation is a very difficult task. This difficulty comes out of two reasons. The first one is connected with establishing of synonymous definition of a damage dimension big enough to be treated as the initial crack. Localization (detection) of the crack tip is the second reason. When the optical method of measurement is used, appearance of the crack can only be established for cracks visible on the outer surface of the specimen. In reality, especially for specimens with Λ-shape notch, the crack can initiate within the invisible part of the specimen. For this reason the supposition on the crack initiation based on the AE measurements seems to be more objective than the standard optical observation*.

Three fundamental stages can be distinguished in the process of fatigue cracking, namely: I. Incubation of the crack. Characteristic features of this stage are the saturation of dislocation structures and arising of the roughnesses on the outer surface; II. Crack growth to the visually perceptible dimensions (initiation); III. Further crack growth (propagation) from the moment of its initial perception to the final destruction of the specimen. The AE method is peculiarly useful in the last two stages. It makes the

---

* Development of new methods of crack measurements observed recently (electromagnetic or electric resistance method) does not change the fact that the optical method is still the most popular one used in practice.

estimation of real initiation of the fatigue crack growth more accurate. It should be noticed that the first optical observation of the crack on the specimen's surface can not be connected with the initiation of the cracking process but it usually indicates that the process is already in progress. It happens also, when the crack tip has been geometrically situated on the visible surface. Precise observation of the moment of crack initiation is usually impossible because the resolving power of optical instruments is not too big and the conditions for observation of the specimen are rather difficult due to its vibrations. On the other hand, just for the reason of specimen vibrations, increase of the resolving power of the optical instruments seems to be aimless.

The acoustic effect produced in the third stage of cracking generally depends on the volume of plastic zone, that is on the length of the crack front and the stress level as well as on the kind of cracking material. The first two factors are important for a given material. In the case of netched specimens with a rectangular cross-section subjected to a cyclic bending with constant amplitude, it can be assumed that at the beginning of cracking, growth of the crack front takes place for constant stresses acting in the cracked region. In this phase increase of AE is connected only with the growth of the crack front length. It happens until the entire specimen's cross-section width is cracked, since from this moment the front length remains constant. It means that now the change of AE depends only of the stress amplitude. In this way correlations between the acoustical effects of tested materials, its fatigue properties and velocity of the crack growth within the structure can be made. The large number of data obtained by measurements is necessary to do it.

Touching the problem of the usefulness of obtained results it should be noticed that the appropriate regulation of the measuring equipment plays a very important role in the AE method [2]. The appropriate total amplification and discrimination levels of the electric signal are the most important factors [2]. Obtained results depend a lot on those parameters and the final success of the experiment is greatly influenced by their proper choice. This problem has been discussed in details in references [1–3] where the results of the AE measurements in the St90PA steel were described.

3. Specimens and testing procedure

Tests were carried out on the normalized carbon-manganese St90PA steel specimens of a following average percentage composition: C 0.68; Mn 1.11; Si 0.24; Cr 0.01; Ni 0.01; Mo 0.10; V 0.02; S 0.027; P 0.026; Fe – the rest. Ultimate strength of this steel equals 1010 MPa and its yield stress is 600 MPa.

The normalized cylindrical specimens with reduced section 5 mm in diameter and 55 mm in gauge length were used for tension. The rectangular specimens were prepared for 3-point bending in three kinds of dimensions: $20 \times 30 \times 250$ mm^3

with straight notch for fatigue crack initiation test; $20 \times 50 \times 220$ mm^3 with Λ-shape notch for fatigue crack propagation, and $20 \times 40 \times 180$ mm^3 with Λ-shape notch according to ASTM E–399–77 for determining fracture toughness and the K_{Ic} factor. Cylindrical specimens were obtained from new railway rails as well as from the 10 years old rails of the railway track, exhibiting the fatigue cracks of a brittle nature. Rectangular specimens descended from the new and exploited rails and a part of the specimens was additionally annealed for 1 hour at the temperature 600°C in open-air conditions and next cooled together with a furnace. Elimination of internal stresses and softening of the material were the basic aims of this heat treatment. Rectangular specimens for a fracture toughness measurements descended only from new rails.

Main investigations were preceded by determination of the AE characteristics of a new and exploited material. These characteristics were obtained for cylindrical specimens stretched to the rupture. Test conditions and obtained results were not different from those described in [1].

Washers were used between the specimen and all the holders or rollers for electric and acoustic isolation of the specimen and for damping of noise of the mechanical nature. Experimental tests were carried out on test stand No. 1 described in [1, 3], that is on the Instron–1251 fatigue testing machine and on the 4 channel AE analyser, type E1, made in Institute of Nuclear Research, Poland. The DZM 180 printer was also used. The AE transducer was located on upper wall of the specimen, in its central part.

The 20 Hz frequency sinusoidally changing loads were used in initiation tests and the 25 Hz frequency was used in other tests. Total amplification of the analyser E1 was 80 dB, its level of discrimination was 1 V and the transmitted frequency band was 65...250 kHz. The high-pass filter used has had the limit frequency equal to 260 Hz. The line printer recorded maximum load value and the AE count rate and count sum. In the AE measurements accompanying the crack initiation the 20 s time base was used, whereas in the measurements of the crack propagation the 1...100 s base was used.

Initiation and growth of the crack length were the additionally inspected and recorded parameters. Stereoscopic optical microscope together with the millimetre mesh marked on both sides of the specimen in the vicinity of the growing crack (or notch) were used in these measurements.

Investigations concerning initiation of a fatigue crack were done for two groups of specimens of the total number of 9. Since such experiments were never carried out before, initially 5 specimens of the pilot group were used in diagnostic investigations. Their basic aim was the appropriate choice of loading parameters and the AE analyser regulation. Estimation of the influence of external disturbances on the measured parameters and the characteristic of the change of these disturbances in time were also the aim of the diagnostic tests. Tests on the main group of specimens done according to the established procedure were the next step of investigations.

4. Results and discussion

Before the beginning of cycling each specimen was quasistatically loaded to $F_{max} = 11.42$ kN with the simultaneous AE recording. The aim of experiment was to check up if the stresses near the notch tip produced by this load were not greater than the yield stress; none of the samples exhibited acoustic activity during this loading. Investigations of the acoustic effects for various load values (Table 1) and the relation of these effects with crack growth were the reason for changing the load. The most important test data are given in Table 2 and Fig. 1. For each specimen it was found that AE produced by cycling was observed much earlier than the crack could be optically discovered on one of the lateral surfaces of the specimen (interval A).

Table 1. Values of cyclic load in particular test intervals

Load \ Test intervals	*A*	*B*	*C*
F_{max} [kN]	11.42	5.30	8.16
F_{min} [kN]	0.80	0.80	0.80
$R = F_{min}/F_{max}$	0.07	0.15	0.10

Table 2. Testing of fatigue crack initiation

Specimen No	Cycle number to appearence/ of intensive AE	Cycle number to optical detection of crack	AE counts to optical detection of crack	Specimen endurance [cycles]	Crack length [mm]	Fatigue crack area [%]
1	2	3	4	5	6	7
1	40 000	50 000	850 000	106 000	2.0	7.3
2	10 200	45 000	461 495	61 500	1.9	7.0
3	18 200	52 000	426 755	58 700	1.9	7.0
4	30 200	52 000	1 342 978	82 600	2.8	10.5
5	33 100	72 000	991 508	86 200	2.0	7.5
6	29 300	63 400	561 500	62 800		
7	21 600	49 500	426 800	60 400		
8	25 500	57 300	860 600	81 600		
9	42 900	65 600	628 900	87 600		

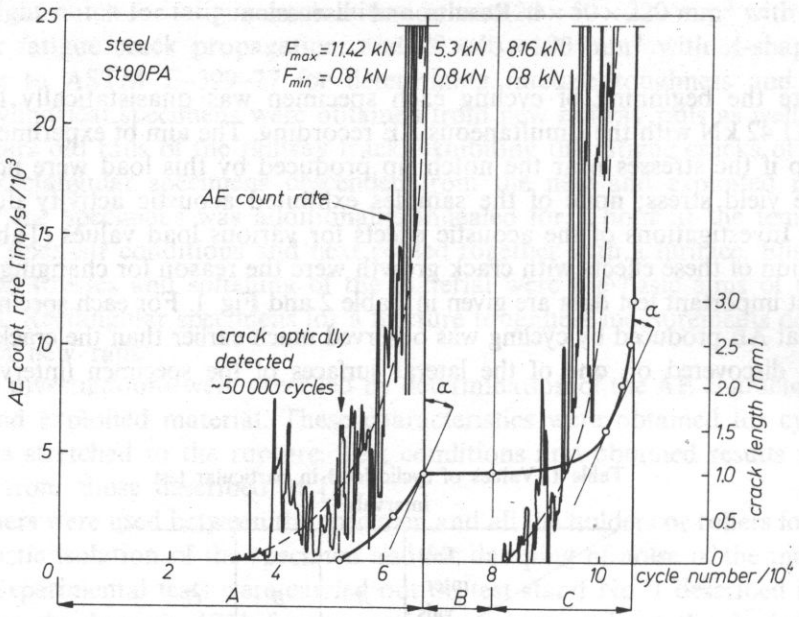

FIG. 1. Acoustic emission count rate and crack length versus cycle number by different load value

If we assume that this activity is produced by crack initiation and its initial growth, then we should say that the acoustic method of detection of appearing cracks is much more effective then the optical method commonly used in practice nowadays. In the successive stage of the process, AE is growing progressively (broken line) together with the crack length growth (solid line).

To investigate AE in the interval B, the maximum cyclic load F_{max} was reduced to 5.30 kN. For this load, AE did not appear. Fatigue crack growth was neither observed, too. This phenomenon was detected every time when F_{max} was reduced. It was observed also in crack propagation tests done for specimens with a Λ-shape notch.

In the interval C the load F_{max} was increased to the value which evoked a distinct AE effect, but which was less by 3.26 kN (about 28%) than in the interval A. Magnification of the specimen's endurance and prolongation of the observation time of a fatigue crack growth together with the accompanying acoustic activity were the reasons for such load changing. When the AE count rate in the interval C reaches the maximum value from the interval A, then the same rate of fatigue crack growth is reached. Direction of tangential lines drawn in the proper points of the crack growth curve indicates for this phenomenon.

Four samples (No. 6 to 9) of the main group were tested for a procedure shown in Fig. 2 (see Sect. 2). Values used in tests were: $F_{max} = 11.2$ kN, $F_{min} = 5.2$ kN, $R = 0.46$. From Figs. 1 and 2 it can be seen that the superiority of the AE method with respect to the optical detection of a fatigue crack initiation is evident.

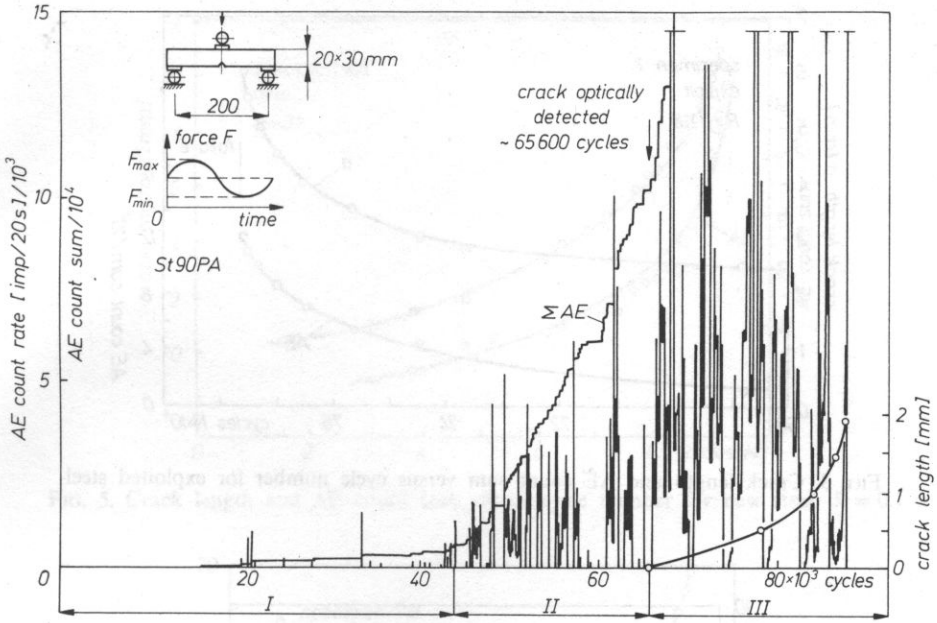

FIG. 2. Acoustic activity of a specimen No. 9 by 3-point cyclic bending

A slightly different procedure was applied in main measurement of the crack propagation. Initial maximum load of a cycle was 24 kN and it was held constant until crack appeared on the lateral surface of the sample. A high initial load was applied in order to reduce the incubation time. The AE measurements conducted in this part of the experiment were only used for qualitative estimation of crack existence. Maximum load was reduced to 14 kN when the crack became visible and could be optically observed on a surface of the sample. Afterwards, both crack development and AE were carefully measured. These results are marked by sample number and a letter *A*. Measurements were conducted to the moment when the crack length reached ca 10 mm. Then load was reduced to 8 kN in order to delay specimen's failure and to obtain second series of results, marked by a letter *B*. For this load, samples were cycled until they were broken; an increment of the crack length attained an average value of 12 mm. Thus, average total crack length reached ca 22 mm. Each change of the maximum load was accompanied by the change in the minimum load of the cycle, because we wanted to keep the assumed value of the stress ratio R constant.

Totally 12 series of measurements for 7 specimens were done. Relations presented in Figs. 3 to 6 were obtained for samples 1, 3*A*, 4*A* and 7*B* in three already mentioned (Section 3) states of the material and for different values of the stress ratio R in the cases when a new material has been used (4*A*, 7*B*). Curves "*a*" for the crack length and "AE" for count sum plotted as the function of load cycles are of the

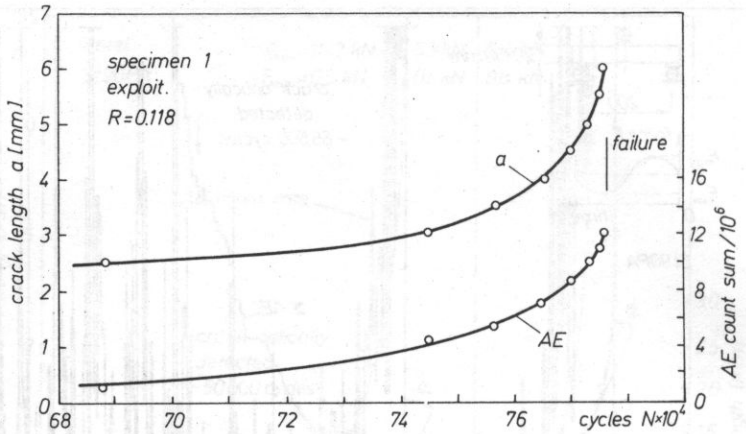

FIG. 3. Crack length and AE count sum versus cycle number for exploited steel

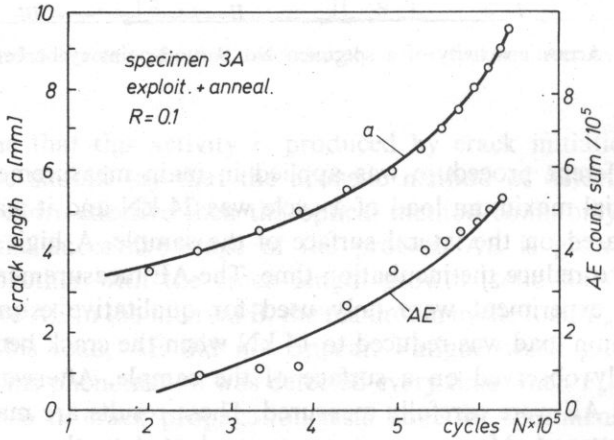

FIG. 4. Crack length and AE count sum versus cycle number for exploited and annealed steel

similar nature, especially by small crack lengths. Differences in the state of the material and in obtained crack lengths can be the reasons for the observed absence of the full parallelism of the curves plotted for greater crack lengths.

Differences which are significant in further interpretation of the obtained results can be observed in the subsequent presentation of the experimental data (see Figs. 7–9). Three characteristic relations between the crack length and the AE counts sum can be distinguished here, namely the linear dependence (Fig. 7, sample 1), the progressively growing nonlinear dependance (Fig. 8, sample 3A) and the regressively growing nonlinear dependance (Fig. 9, sample 4A).

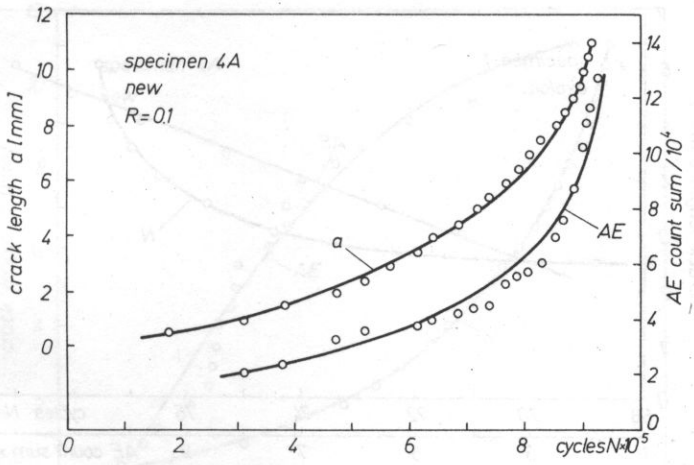

FIG. 5. Crack length and AE count sum versus cycle number for new steel, $R = 0.1$

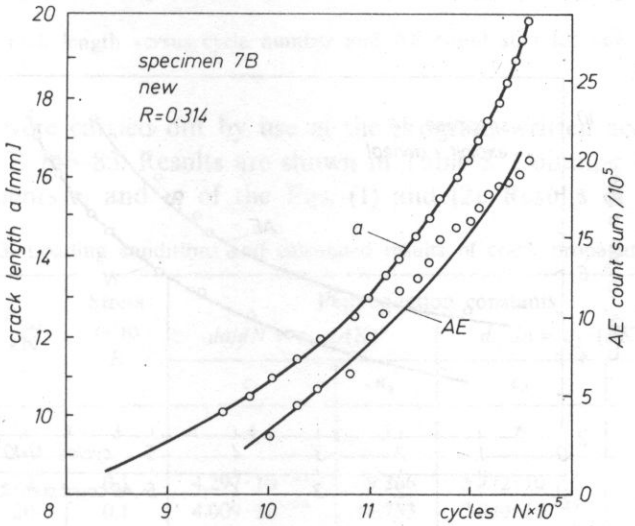

FIG 6. Crack length and AE count sum versus cycle number for new steel, $R = 0.314$

We can notice that there is a certain relation between the crack length and the AE count sum. This relation can be seen in both coordinate systems: crack length and the count sum as a function of the number of cycles as well as crack length as a function of the AE count sum and number of cycles. In accordance with this relation the count sum can be treated as a parameter of the meaning similar to the number of load cycles. The well known Paris' equation for crack growth rate reads as follows.

$$da/dN = c_1(\Delta K)^{n_1}, \tag{1}$$

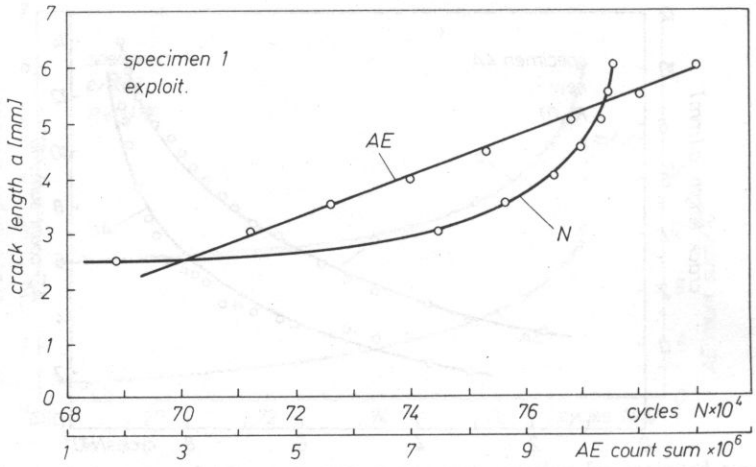

FIG. 7. Crack length versus cycle number and AE count sum for explited steel

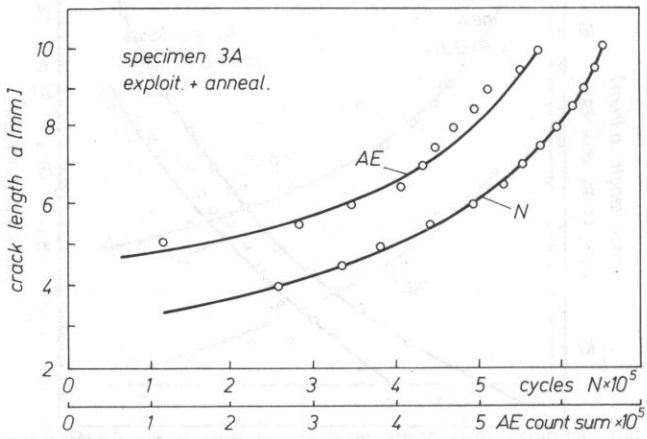

FIG. 8. Crack length versus cycle number and AE count sum for explited and annealed steel

where da/dN – increment of fatigue crack per cycle, c_1, n_1 – material constants, ΔK – range of the stress intensity factor.

It seems to be reasonable to use a similar formula for describing the crack growth in terms of AE parameters

$$da/dn = c_2(\Delta K)^{n_2}, \tag{2}$$

where da/dn – increment of fatigue crack per AE count.

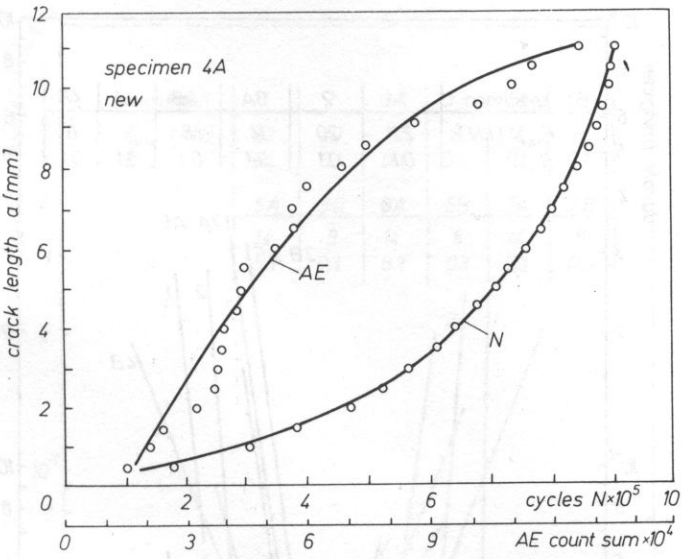

FIG. 9. Crack length versus cycle number and AE count sum for new steel

Calculations were carried out by use of the program written according to the standard ASTM E 746–83. Results are shown in Table 3. Columns 4 to 7 give the estimated coefficients c_i and n_i of the Eqs. (1) and (2). Results of the numerical

Table 3. Loading conditions and calculated results of crack propagation

No	F_{max} kN	Stress ratio R	Paris'equation constants $da/dN = c_1 \cdot (\Delta K)^{n_1}$		$da/dn = c_2 \cdot (\Delta K)^{n_2}$	
			c_1	n_1	c_2	n_2
1	2	3	4	5	6	7
1^e	22	0.1	$4.297 \cdot 10^{-21}$	9.266	$5.772 \cdot 10^{-17}$	4.650
2^e	20	0.1	$4.009 \cdot 10^{-24}$	11.753	$3.840 \cdot 10^{-25}$	10.709
$3A^a$	14	0.1	$5.667 \cdot 10^{-18}$	7.132	$3.005 \cdot 10^{-18}$	6.492
$3B^a$	8	0.1	$2.593 \cdot 10^{-18}$	7.919	$3.377 \cdot 10^{-16}$	4.977
$4A^n$	14	0.1	$2.939 \cdot 10^{-13}$	3.829	$3.501 \cdot 10^{-2}$	−4.262
$4B^n$	8	0.1	$4.124 \cdot 10^{-12}$	2.981	$3.901 \cdot 10^{-3}$	−3.756
$5A^n$	14	0.3	$3.088 \cdot 10^{-11}$	2.542	$7.227 \cdot 10^{-18}$	6.778
$5B^n$	8	0.3	$1.983 \cdot 10^{-10}$	1.780	$7.780 \cdot 10^{-13}$	2.045
$6A^n$	14	0.3	$3.172 \cdot 10^{-11}$	2.567	—	—
$6B^n$	8	0.3	$5.806 \cdot 10^{-12}$	3.062	—	—
$7A^n$	14	0.3	$3.102 \cdot 10^{-11}$	2.606	$1.070 \cdot 10^{-12}$	2.140
$7B^n$	8	0.3	$5.544 \cdot 10^{-11}$	2.262	$9.813 \cdot 10^{-12}$	2.198

(ᵉ) Exploited steel.
(ᵃ) Exploited and annealed steel.
(ⁿ) New steel.

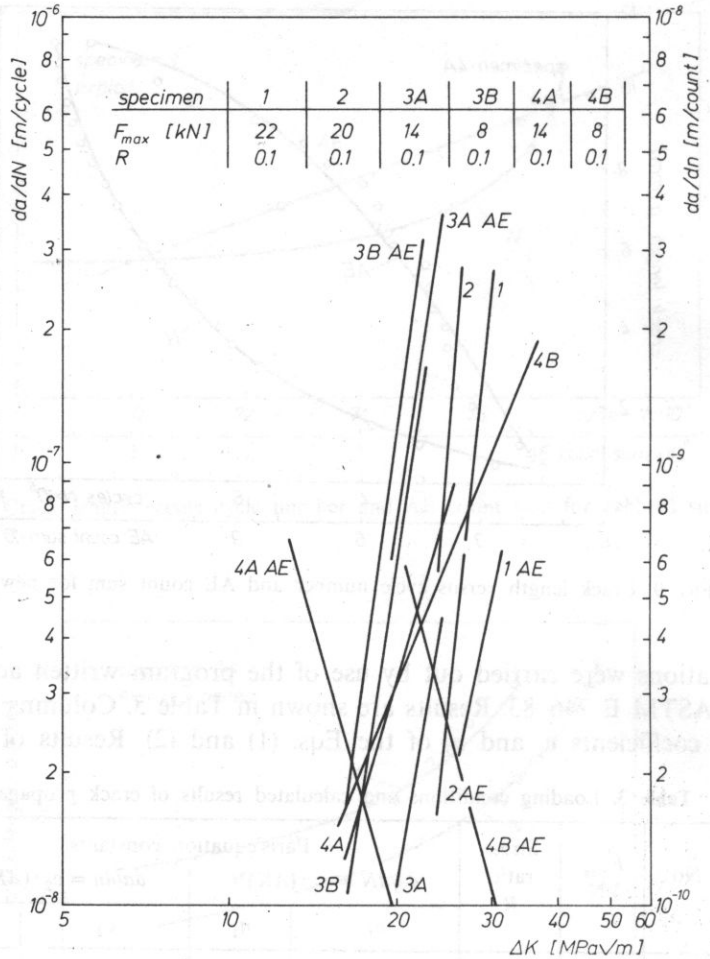

FIG. 10. da/dN and da/dn versus ΔK

analysis are plotted in the doubly logarithmic system in Figs. 10 and 12. They form the most synthetic picture of the results obtained by our measurements. Fig. 10 shows that the AE estimations are in a good conformity with the results obtained with the use of fracture mechanics methods. Nonconformity of the load cycles with the AE count per unit increment of crack length is the reason that explains the shifting of corresponding lines 1 – 1AE, 2 – 2AE, 3A – 3A AE, 3B – 3B AE, etc. It should be noticed that 10 to 100 of the AE counts correspond to one load cycle. Presented results also suggest that the value of load applied for the constant stress ratio R (see Table 3) does not influence the conformity of acoustical and mechanical results.

Results obtained for the specimen No. 4 (new railway rail) are not similar (Fig.

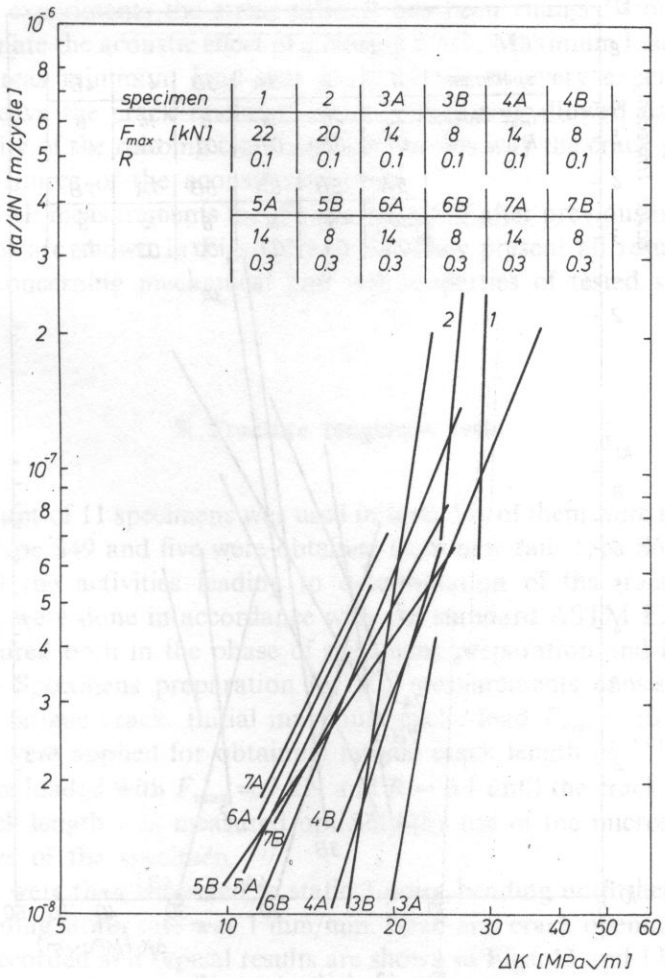

FIG. 11. da/dN versus ΔK

10). Although loading conditions applied here have been the same as in the specimen 3, AE measurements are qualitatively different. This difference is invisible when the relation between crack length and the number of load cycles of Fig. 5 is considered. It becomes evident both for the relation expressing the increment of crack length as a function of AE count sum (see the regressively growing "AE" curve from Fig. 9) and for the results of numerical analysis. Straight lines 4A–AE and 4B–AE in Fig. 10 are descending lines (they have inverse inclination). This result seems to be illogical when the fracture mechanics viewpoint is applied. Relation $da/dN = c_1(\Delta K)^{n_1}$ can be represented in a double logarithmic system by a straight line inclined with respect to

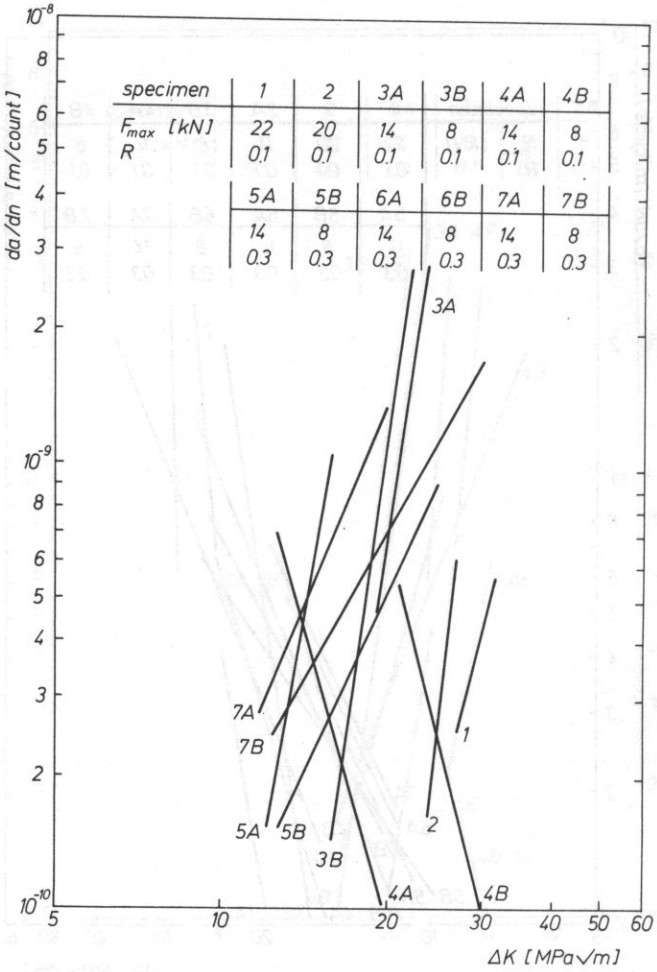

FIG. 12. *da/dn* versus ΔK

the ΔK axis by an angle less than 90°. It follows from the rule that stress increments are usually accompanied by a growth of the fatigue crack propagation velocity but the inverse statement is never true. When *da/dn* is measured, it can sometimes happen that crack length growth implies growth of *dn/da*, that is growth of the count number per unit crack length increment and the decrease of *da/dn*. This result can be explained if we assume that there exists an additional AE source. Acoustic activity of this source grows with fatigue crack length growth. Friction occurring on newly created surfaces in crack opening and closure can be regarded as this additional source. Activity of this source can be much greater than activity of sources directly connected with crack growth, that is with expansion of a plastic zone near the crack tip and with creation of a new surface.

In further experiments the stress ratio R has been changed from 0.1 to 0.3 in order to eliminate the acoustic effect of a closing crack. Maximum load of a cycle was constant whereas minimum load was made higher in every experiment. It gave occasion to leave the crack unclosed in unloading and allowed us to reduce the acoustic activity of the rubbing crack surfaces. In this way the crack growth was the predominant source of the acoustic emission.

Results of AE measurements for the specimen 5–7 after previous magnification of the stress ratio are shown in Figs. 11 and 12. They present all results obtained in experiments concerning mechanical and AE properties of tested specimens.

5. Fracture toughness tests

Total amount of 11 specimens was used in tests. Six of them were made from new railway rails type S49 and five were obtained from new rails type S60 with thermal treatment. All the activities leading to determination of the fracture toughness coefficient K_{Ic} were done in accordance with the standard ASTM E399. Moreover, AE was measured both in the phase of specimens preparation and in the phase of their fracture. Specimens preparation for K_{Ic} measurements consisted in making a preliminary fatigue crack. Initial maximum cyclic load $F_{max} = 10$ kN nad stress ratio $R = 0.1$ were applied for obtaining fatigue crack length of $3^{\pm 1}$ mm and then specimens were loaded with $F_{max} = 7$ kN and $R = 0.1$ until the crack length reached $5^{\pm 1}$ mm. Crack length was measured optically (by use of the microscope) on both lateral surfaces of the specimen.

Specimens were then subjected to static 3-point bending until their final fracture occurred. Bending strain rate was 1 mm/min. Load and crack opening displacement (COD) were recorded and typical results are shown in Figs. 13 and 14. Fig. 15 shows surface of specimens 27 and 28. Majority of obtained fractures is of the same nature as for the specimen No. 27. An important feature of the fracture is its shape and position of a boundary between extemporary and fatigue regions. It should have a shape of a straight line and it should be symmetric with respect to the axis of symmetry of a cross-section. Fracture obtained for the specimen 28 is the example of the improper boundary between these two regions, as it is inclined and bent.

Linear dependence of the crack opening and the applied load and step increment of crack length by the load F_Q has been observed for all tested specimens except the specimen 27 (cf Fig. 14a), where points F_Q and F_{max} coincided. Specimens from rails without heat treatment fractured with much higher crack opening than specimens with heat treatment. Mean crack opening typical for the first case was ca 0.32 mm whereas in the second case it was ca 0.16 mm.

This retardation in fracture of specimens without a heat treatment is represented in Fig. 13 by the curve segment between points F_{max} and K. Moreover, one or even

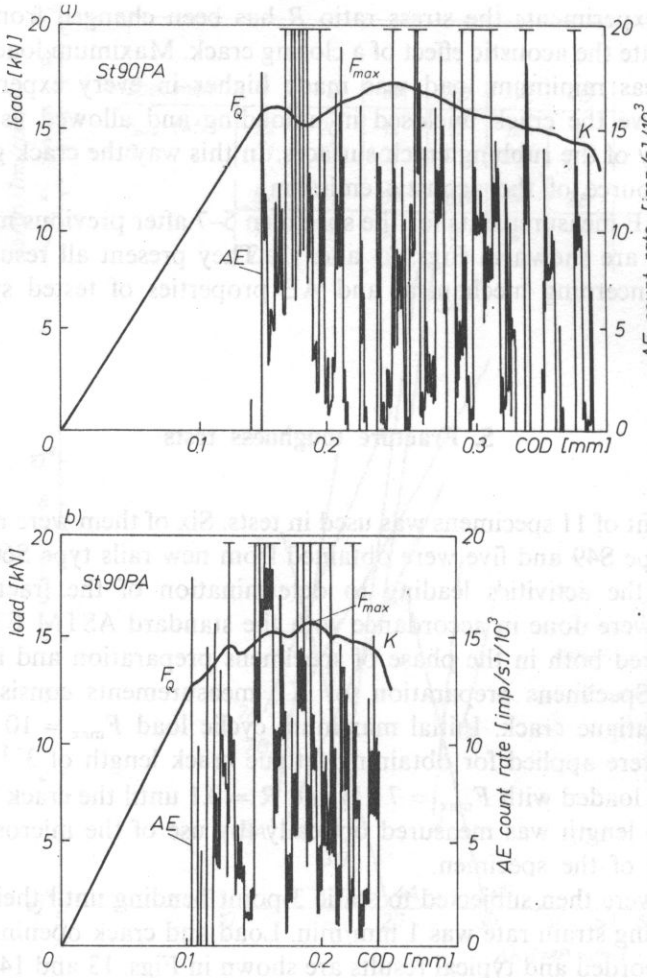

FIG. 13. Bending load value and AE count rate versus COD (rail type S49)

more distinct minima can be seen for specimens made from S49 rails. Curves plotted for specimens made from S60 rails did not exhibit this feature. These differences, except the calculated values of K_{IC}, allow us to distinguish both materials with regard to their inclination to brittle fracture.

Differentiation of both materials with respect to their brittle fracture toughness seems to be even more evident when measurements of the AE counts are taken into account. Specimens made from rails without heat treatment, in spite of different shape of their load curve (Fig. 13), exhibit acoustic activity in fracture contained between points F_Q and K. The most important result of the AE measurement is the coincidence of the beginning of acoustic activity with the initiation of crack growth. Both processes had begin in point F_Q. In this way the AE result confirms the

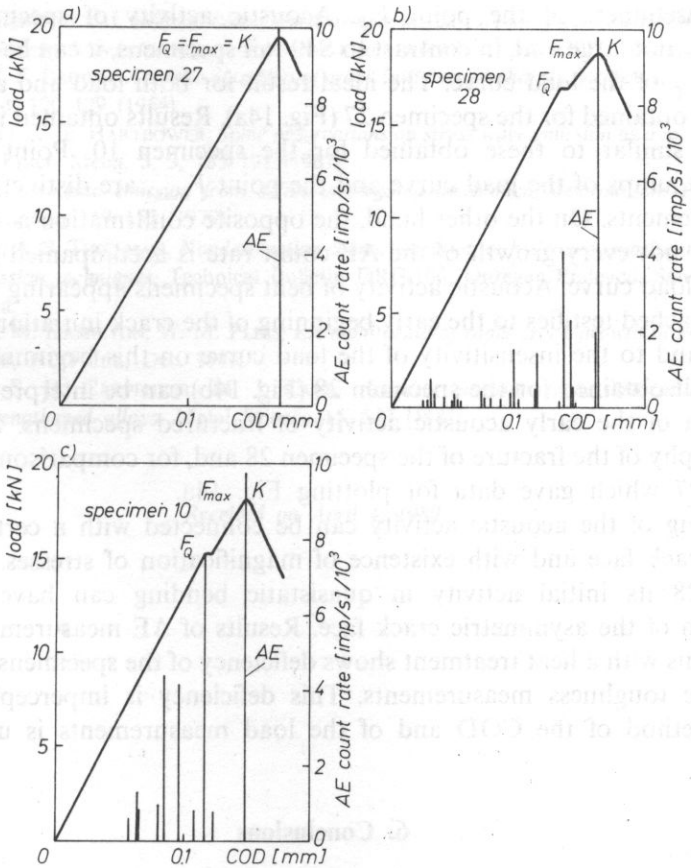

FIG. 14. Bending load value and AE count rate versus COD (rail type S60, annealed)

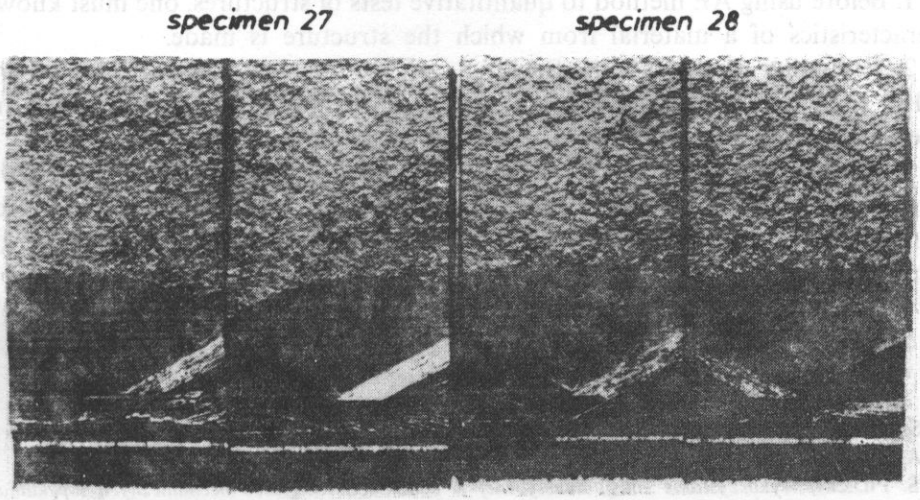

FIG. 15. Fracture surface of fatigued specimens. Boundary between extemporary and fatigue regions is well visible

practical usefulness of the point F_Q. Acoustic activity of specimens with heat treatment is not large and, in contrast to S49 rail specimens, it can be observed below the point F_Q of the load curve. The ideal result for both load and acoustic activity curves was obtained for the specimen 27 (Fig. 14a). Results obtained in the remaining tests were similar to these obtained for the specimen 10. Point F_Q as well as subsequent jumps of the load curve and the point F_{max}, are distinctly confirmed by AE measurements. On the other hand, the opposite confirmation is not observed. It means that not every growth of the AE count rate is accompanied by a significant step of the load curve. Acoustic activity of bent specimens appearing before point F_Q has been reached testifies to the early beginning of the crack initiation process on the one hand and to the insensitivity of the load curve on this beginning on the other hand. Result obtained for the specimen 28 (Fig. 14b) can be interpreted as a certain explanation of the early acoustic activity of fractured specimens. Fig. 15a shows a photography of the fracture of the specimen 28 and, for comparison, fracture of the specimen 27 which gave data for plotting Fig. 14a.

Beginning of the acoustic activity can be connected with a certain features of a fatigue crack face and with existence of magnification of stresses. In the case of specimen 28 its initial activity in quasistatic bending can have its source in equalization of the asymmetric crack face. Results of AE measurements conducted for specimens with a heat treatment shows deficiency of the specimens preparation to the fracture toughness measurements. This deficiency is imperceptible when the classical method of the COD and of the load measurements is used.

6. Conclusions

Results of the presented experiments show that

1. Before using AE method to quantitative tests of structures, one must know AE characteristics of a material from which the structure is made.

2. Beginning of the fatigue cracking can be discovered by AE method much earlier than by optical method, and crack growth rate can be estimated more precisely.

3. AE measurements can be helpful in precise estimation of crack length.

4. AE method is able to make an estimation of fracture toughness more precise than optical method and it can indicate when cracking of particular microregions occurs.

References

[1] S. PILECKI, J. SIEDLACZEK, *Acoustic activity of some metals determined by the acoustic emission method*, Arch. of Acoust. **14**, 3–4, 261–281 (1989).

[2] S. PILECKI, *Wykorzystanie emisji akustycznej w badaniach własności mechanicznych i pękania ciał stałych*, Arch. Akust. **21**, 109 (1986).

[3] S. PILECKI, J. SIEDLACZEK, I. JAROSZYŃSKA, *Opracowanie metody wykorzystania emisji akustycznej do oceny inicjacji kruchych pęknięć szyn kolejowych i ram wózków*. PAN IPPT. Warszawa 1984.

[4] H. M. JONES, W. F. BROWN, *Acoustic detection of crack initiation in sharply notched specimens*, Mater. Res. Stand. **4**, 3, 120–129 (1964).

[5] W. W. GERBERICH, C. E. HARTBOWER, *Some observations on stress wave emission as a measure of crack growth*. Int. J. Fract. Mech. **3**, 3, 185–191 (1967).

[6] A. A. POLLOCK, *Acoustic emission from solids undergoing mechanical deformation*, Ph. D. thesis, University of London 119–157 (1970).

[7] H. L. DUNEGAN, A. S. TETELMAN, *Nondestructive characterization of hydrogen-embrittlement cracking by acoustic emission techniques*, Technical Bulletin DRC-106, Duregan/Endevco, San Juan Capisfrano, California.

[8] C. D. BAILEY, I. M. HAMILTON, W. M. PLESS, *EA monitoring of rapid crack growth in production-size wing fatigue test*, NDT Int., Dec. 1976.

[9] C. R. HEIPLE, S. H. CARPENTER, M. J. CARR, *Acoustic emission from dislocation motion in precipitation-strengthened alloys*, Metal Science 15, 587 (1981).

Received on April 4, 1989